Check for updates

Multiple signaling pathways induced by hexavalent, monospecific, anti-CD20 and hexavalent, bispecific, anti-CD20/CD22 humanized antibodies correlate with enhanced toxicity to B-cell lymphomas and leukemias

Pankaj Gupta,[1] David M. Goldenberg,[2] Edmund A. Rossi,[3] and Chien-Hsing Chang[1,3]

[1]Immunomedics Inc, Morris Plains, NJ; [2]Garden State Cancer Center, Center for Molecular Medicine and Immunology, Belleville, NJ; and [3]IBC Pharmaceuticals, Morris Plains, NJ

We have generated hexavalent antibodies (HexAbs) comprising 6 Fabs tethered to one Fc of human IgG1. Three such constructs, 20-20, a monospecific HexAb comprising 6 Fabs of veltuzumab (humanized anti-CD20 immunoglobulin G1κ [IgG1κ]), 20-22, a bispecific HexAb comprising veltuzumab and 4 Fabs of epratuzumab (humanized anti-CD22 IgG1κ), and 22-20, a bispecific HexAb comprising epratuzumab and 4 Fabs of veltuzumab, were previously shown to inhibit proliferation of several lymphoma cell lines at nanomolar concentrations in the absence of a crosslinking antibody. We now report an in-depth analysis of the apoptotic and survival signals induced by the 3 HexAbs in Burkitt lymphomas and provide in vitro cytotoxicity data for additional lymphoma cell lines and also chronic lymphocytic leukemia patient specimens. Among the key findings are the significant increase in the levels of phosphorylated p38 and phosphatase and tensin homolog deleted on chromosome 10 (PTEN) by all 3 HexAbs and the notable differences in the signaling events triggered by the HexAbs from those incurred by crosslinking veltuzumab or rituximab with a secondary antibody. Thus, the greatly enhanced direct toxicity of these HexAbs correlates with their ability to alter the basal expression of various intracellular proteins involved in regulating cell growth, survival, and apoptosis, with the net outcome leading to cell death. (*Blood*. 2010;116(17):3258-3267)

Introduction

To address the clinical concerns of undesirable immmunogenicity and suboptimal pharmacokinetics, cancer therapy with monoclonal antibodies (mAbs) has evolved from murine to chimeric, humanized, and now fully human constructs. Parallel to these improvements have been continuing efforts to develop more effective forms of mAbs, which to date, include different isotypes, smaller single-chain proteins with monomeric or multimeric binding moieties derived from variable domains, specific mutations in the Fc to modulate immune effector functions or circulating half-lives, and bispecific antibodies (bsAbs) of numerous designs that vary in valency, structure, and constituents, among others.[1]

In the absence of a covalently attached drug, toxin, or radionuclide, the toxicity of a mAb after ligation of its cognate antigen on target cells can be either direct or indirect. Direct toxicity is caused primarily by apoptosis, resulting from perturbation of intracellular signal transduction pathways, whereas indirect toxicity requires the involvement of effector cells and complement, which lead to antibody-dependent cellular cytotoxicity (ADCC), complement-dependent cytotoxicity (CDC), and/or monocyte/macrophage phagocytosis. Despite this variety of mechanisms of action, most mAbs are not administered as a monotherapy, but usually are combined with other modalities, particularly chemotherapy. Because signaling pathway redundancies can result in lack of response to a single mAb, diverse strategies to use 2 mAbs, each against a different epitope of the same antigen or different antigens on the same target cell, have been proposed, and combinations such as anti-CD20 and anti-CD22,[2] anti-CD20 and anti–human leukocyte antigen DR,[3] anti-CD20 and anti-TRAIL-R1,[4] anti-insulin–like growth factor 1 receptor (IGF-1R) and anti–epidermal growth factor receptor (EGFR),[5] anti–IGF-1R and anti–vascular endothelial growth factor,[6] or trastuzumab and pertuzumab that target different extracellular regions of human epidermal growth factor receptor 2[7] have been evaluated preclinically, showing enhanced or synergistic antitumor activity both in vitro and in vivo.

The first clinical evidence of an apparent advantage of combining 2 mAbs against different cell surface antigens of a cancer cell involved the administration of rituximab, the chimeric anti-CD20 mAb, and epratuzumab, the humanized anti-CD22 mAb, in patients with non-Hodgkin lymphoma (NHL), where the combination was found to enhance antilymphoma efficacy without a commensurate increase in toxicities, based on 3 independent clinical trials.[8] A bsAb targeting both EGFR and IGF-R has been studied,[9] yet the combination of the 2 parental mAbs has not been reported to be additive or synergistic. Given the short list of mAbs currently approved in cancer therapy, the available combinations are not large. Nevertheless, where such combinations show improved efficacy, it is of concern, from an economic perspective, whether the costs of combining 2 expensive antibody therapies can be borne by the healthcare system, in addition to the inconvenience and time of conducting separate infusions. Therefore, developing bsAbs, whereby 2 antigen targets can be bound by a single agent, has been a goal for some time, resulting in a multitude of approaches.[10]

Earlier methods used for the production of bsAbs made use of either chemical cross-linking of IgG or Fab′[11,12] or quadromas[13]

Submitted March 30, 2010; accepted June 19, 2010. Prepublished online as *Blood* First Edition paper, July 13, 2010; DOI 10.1182/blood-2010-03-276857.

The publication costs of this article were defrayed in part by page charge payment. Therefore, and solely to indicate this fact, this article is hereby marked "advertisement" in accordance with 18 USC section 1734.

© 2010 by The American Society of Hematology

Downloaded from http://ashpublications.net/blood/article-pdf/116/17/3258/1331735/zh804310003258.pdf by guest on 24 May 2024

obtained by fusing 2 hybridomas. Subsequent strategies focused on generating recombinant bsAbs composed of tandem scFvs or diabodies,[14] and one format of such Fc-lacking constructs, referred to as BiTe, is currently being tested clinically.[15] Because, for many therapeutic applications, the presence of an Fc and its effector functions is beneficial, if not essential, for improved in vivo properties, Fc-containing bsAbs, as exemplified by a variety of novel designs, also have been described.[16-20] Indeed, a renewed interest in the construction of IgG-like bsAbs has emerged[21] to recruit effector cells, which is an important mechanism for most of the currently available anticancer mAbs.

We have advanced a new approach of constructing multivalent antibodies using the Dock-and-Lock (DNL) method,[22] which enables site-specific self-assembly of 2 modular components only with each other, resulting, after combining, in a covalent structure of defined composition with retained bioactivity.[23] With the available DNL method and noting that the administration of both anti-CD20 and anti-CD22 antibodies showed improved antilymphoma efficacy without increased toxicity in patients,[8,24] as well as enhanced activity in a lymphoma xenograft model,[2] we embarked on the generation of a pair of bispecific anti-CD20/CD22 hexavalent antibodies (HexAbs), designated 22-20 and 20-22, each consisting of an immunoglobulin G (IgG) linked to 4 additional Fabs.[25] Specifically, 22-20 comprises epratuzumab and 4 Fabs of veltuzumab, and 20-22 comprises veltuzumab and 4 Fabs of epratuzumab. In addition, a monospecific anti-CD20 HexAb, 20-20, comprising 6 Fabs of veltuzumab, was constructed and evaluated.[26] We found that 22-20, 20-22, and 20-20 have distinct properties compared with their parental counterparts, including enhanced antilymphoma activity in vitro and comparable efficacy in vivo, despite showing shorter circulating half-lives.[25,26]

The goal of this study was to extend our in vitro characterization of 20-20, 20-22, and 22-20, with a primary interest in elucidating the intracellular signaling pathways involved in transducing CD20 upon ligating human lymphoma cells with each of these 3 HexAbs, and comparing the results with those obtained in parallel with epratuzumab, veltuzumab, and rituximab. Selective experiments were performed to determine whether the individual profile of the kinase activated by the anti-CD20/CD22 HexAbs would be similar to or different from that triggered by anti-IgM, or by crosslinking veltuzumab or rituximab with a secondary antibody. The data presented here allow us to correlate the enhanced direct cytotoxicity of the anti-CD20/CD22 HexAbs, compared with their bivalent parental antibodies, with their increased ability to up-regulate PTEN (phosphatase and tensin homology deleted on chromosome 10), phosphorylated p38, and cyclin-dependent kinase (CDK) inhibitors, as represented by p21, p27, and Kip2. The reasons for selecting 22-20 as the best lead among the 3 HexAbs for clinical evaluation also are discussed.

Methods

Antibodies and reagents

The generation and preparation of 20-20, 20-22, and 22-20 have been described previously.[25,26] Rituximab was obtained from commercial supplies. Mouse antihuman IgM was purchased from Southern Biotech. Other antibodies were from Cell Signaling or Santa Cruz Biotechnology. Horseradish peroxidase–conjugated secondary antibodies were obtained from Jackson ImmunoResearch Laboratories. Heat-inactivated fetal bovine serum was purchased from Hyclone. Cell culture media, supplements, tetramethylrhodamine ethyl ester, and the transfection reagent DMRIE-C were bought from Invitrogen Life Technologies. One Solution MTS [3-(4,5-dimethylthiazol-2-yl)-5-(3-carboxymethoxyphenyl)-2-(4-sulfophenyl)-2H-tetrazolium] assay reagent was obtained from Promega. Reducing 4%-20% gradient Tris-glycine gels were from Cambrex Bio Science. Annexin V–Alexa Fluor 488 conjugate for apoptosis detection was obtained from Invitrogen. All other chemicals were purchased from Sigma-Aldrich.

Cell culture

Burkitt (Daudi, Raji) and non-Burkitt (RL and DoHH2) human lymphoma lines were obtained from ATCC and cultured at 37°C in 5% CO_2 and RPMI 1640 medium supplemented with 10% heat-inactivated fetal bovine serum, 2mM L-glutamine, 200 U/mL penicillin, and 100 μg/mL streptomycin. Cells from chronic lymphocytic leukemia (CLL) patients were collected from whole blood by Ficoll-Hypaque separation[27] and grown in RPMI media as described above. All patients gave written informed consent in accordance with the Declaration of Helsinki under an approved protocol of the Institutional Review Board of Weill-Cornell Medical College (New York, NY).

Cell viability assay

Cells were seeded at a density of 1×10^5 cells/mL in 96-well plates (1×10^4 cells/well) and incubated with each test Ab at a final concentration of 0.01-500nM for 3 (Daudi) and 4 days (Raji, RL, and DoHH2). Where indicated, Abs were cross-linked with a secondary goat anti–human (GAH) Ab at a concentration of 10 μg/mL. Patient CLL cells were seeded in 48-well plates at a density of 5×10^5 cells/mL (1.5×10^5 cells/well) and incubated with each test Ab at a final concentration of 10nM for 3 days. The number of living cells was then determined using the soluble tetrazolium salt MTS following the manufacturer's protocol.

Annexin V binding assay

Cells in 6-well plates (2×10^5 cells/well at 1×10^5 cells/mL) were treated with each test Ab at 10 or 100nM for 24 hours, washed, resuspended in 100 μL of annexin-binding buffer (10mM HEPES [N-2-hydroxyethylpiperazine-N′-2-ethanesulfonic acid], 140mM NaCl, and 2.5mM $CaCl_2$ in phosphate-buffered saline; PBS), stained with 5 μL of annexin V–Alexa Fluor 488 conjugate for 20 minutes, followed by staining with 1 μg/mL of propidium iodide (PI) in 400 μL of annexin-binding buffer, and analyzed by flow cytometry (FACSCalibur; Becton Dickinson). Cells stained positive with annexin V (including both PI-negative and -positive) were counted as apoptotic populations.

Cell-cycle analysis

Cells were seeded and treated with each test Ab as described for the annexin V binding assay, except that they were resuspended in 0.5 mL of a solution containing PI (50 μg/mL), sodium citrate (0.1%), and Triton X-100 (0.1%) and stained for 1 hour before analysis by flow cytometry.

Assessment of mitochondrial membrane depolarization

Changes in mitochondrial transmembrane potential ($\Delta\psi_m$) were determined by flow cytometry. Briefly, Daudi cells in 6-well plates (2×10^5 cells/well seeded at 1×10^5 cells/mL) were incubated overnight (16 hours) with rituximab (133nM), veltuzumab (133nM), or each of the 3 HexAbs (100nM). Samples also included rituximab (133nM) or veltuzumab (133nM) in the presence of a crosslinking antibody (10 μg/mL). Cells were stained for 30 minutes in the dark at 37°C with 50nM of the fluorescent probe tetramethylrhodamine ethyl ester in a medium containing antibiotics and serum, washed 3× with PBS, and analyzed.

Immunoblot analysis

In general, Daudi or Raji cells (1×10^6 cells/mL) were treated for a predetermined time with rituximab, veltuzumab, or epratuzumab at 133 or 10nM, or with 20-20, 20-22, or 22-20 at 10nM, then washed in PBS, centrifuged, and lysed in ice cold 1× RIPA buffer comprising 2mM sodium

Downloaded from http://ashpublications.net/blood/article-pdf/116/17/3258/1331735/zh804310003258.pdf by guest on 24 May 2024

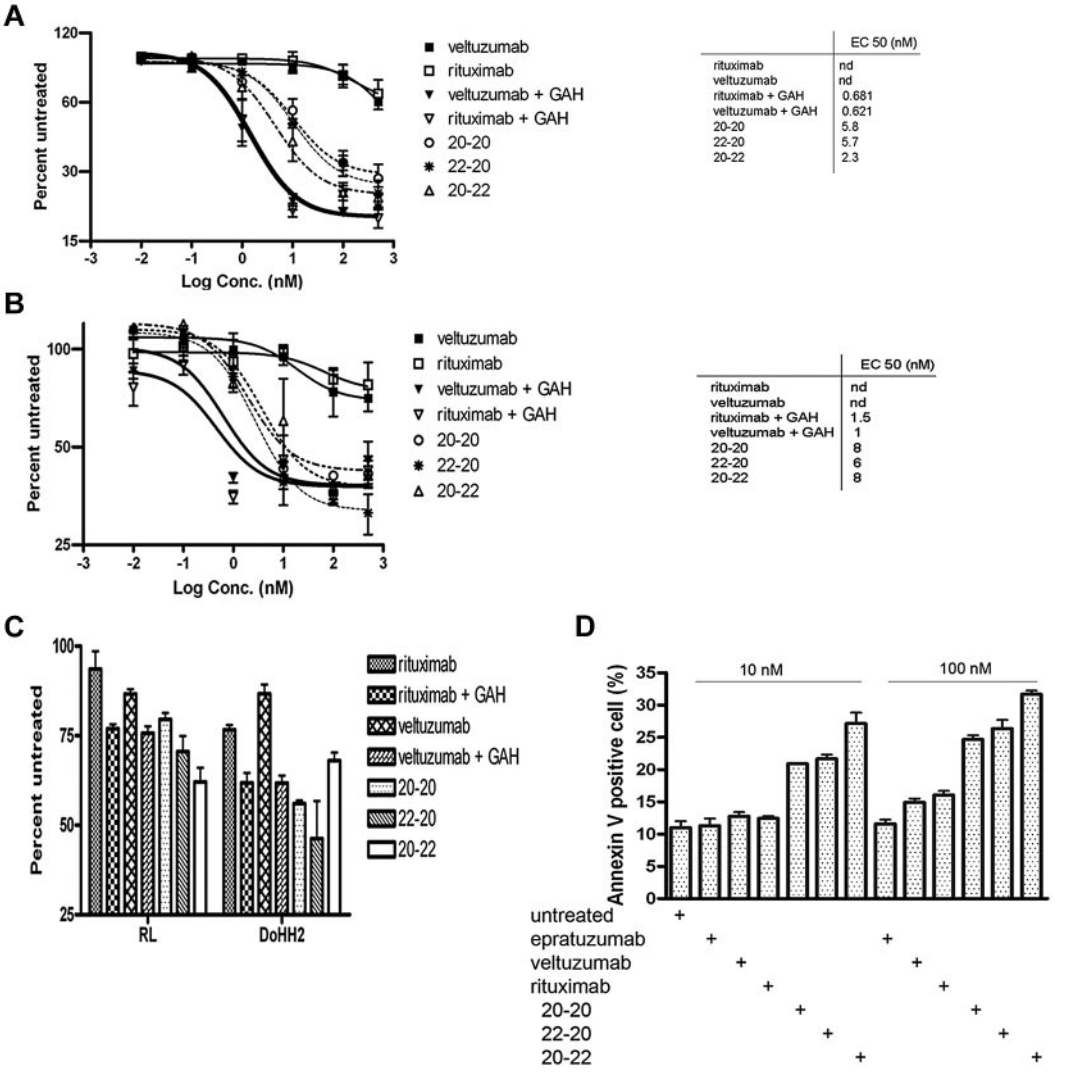

Figure 1. In vitro cytotoxicity as determined by the MTS assay and apoptosis by the annexin V staining. Shown are results for Daudi (A), Raji (B), RL and DoHH2 (C), and the annexin V binding assay for Daudi (D). The concentrations of each primary antibody and GAH (C) were 10nM and 10 μg/mL, respectively.

orthovanadate, 5mM sodium fluoride, 2.5mM sodium pyrophosphate, 1mM β-glycerophosphate, and 0.25% sodium deoxycholate. The lysates were centrifuged at 13 000*g*, and the supernatants were collected. Protein content was determined using the protein assay kit from Bio-Rad, with bovine serum albumin as the standard. Protein samples (25 μg) were mixed with the lysis buffer and heated at 95°C for 5 minutes, followed by separation on 4%-20% gradient Tris-glycine gels. Separated proteins were transferred electrophoretically onto nitrocellulose membranes (Bio-Rad). Nonspecific binding sites were blocked in 10mM Tris-buffered saline containing 0.05% Tween-20 (TBS-T) and 10% nonfat milk. Membranes were incubated with a primary antibody (1:1000 dilution in TBS-T containing 5% bovine serum albumin) overnight at 4°C. The next day, membranes were washed 3× with TBS-T at room temperature. Horseradish peroxidase–conjugated secondary antibody (1:5000 dilution) was used to probe the primary antibody. Blots were visualized with enhanced chemiluminescence (Thermo Scientific).

RNA interference of PTEN

Daudi cells were transfected with PTEN small interfering RNA (siRNA; Cell Signaling Technologies) or control siRNA (Santa Cruz Biotechnology) in 6-well plates using DMRIE-C, per manufacturer's instructions, then treated with each HexAb at 10nM for 16 hours. Cells were washed with PBS, stained with annexin V conjugate for 20 minutes, and analyzed by flow cytometry. Controls also included cells incubated with only DMRIE-C. Immunoblot analysis was performed as described above with 5-μg protein samples and anti-PTEN antibody.

Results

Growth inhibition and apoptosis

The dose-response curves (Figure 1A) obtained with the MTS assay from a 3-day treatment of Daudi cells indicated comparable values of EC_{50} for 20-20, 22-20, and 20-22 (2.3-5.8nM), which were 100-fold lower (ie, more potent) than veltuzumab or rituximab (> 500nM). Under these conditions, crosslinking veltuzumab or rituximab with GAH Ab potently inhibited the proliferation of Daudi cells, with an EC_{50} of approximately 0.6nM. Previous results[25] obtained from a cell counting assay at day 5 in Daudi demonstrated lower EC_{50} values for 22-20 (0.32nM) and 20-22 (0.5nM), which may have been due to a longer incubation time (5 vs 3 days), as well as using a different assay (cell counting vs MTS). The 3 HexAbs also inhibited the proliferation of Raji (Figure 1B), with EC_{50} values of 6-8nM, and when tested at 10nM,

Downloaded from http://ashpublications.net/blood/article-pdf/116/17/3258/1331735/zh804310003258.pdf by guest on 24 May 2024

Table 1. Cytotoxicity of HexAbs on CLL patient specimens as determined by the MTS assay

Patient ID	CD20 expression	Rituximab	Rituximab +GAH	Veltuzumab	Veltuzumab+GAH	20-20	22-20	20-22
CLL021	Low	114 ± 6	120 ± 6	113 ± 12	103 ± 11	117 ± 2	118 ± 6	114 ± 4
CLL022	Low	102 ± 5	107 ± 5	106 ± 1	102 ± 3	114 ± 1	113 ± 1	99 ± 2
CLL030	Low	107 ± 2	105 ± 2	105 ± 3	105 ± 16	108 ± 3	115 ± 2	104 ± 3
CLL037	Low	107 ± 5	102 ± 18	102 ± 8	90 ± 4	109 ± 4	99 ± 3	96 ± 6
CLL078	Moderate	104 ± 1	98 ± 2	101 ± 3	93 ± 4	74 ± 5	76 ± 1	72 ± 2
CLL113	High	101 ± 1	97 ± 4	92 ± 1	96 ± 3	45 ± 2	43 ± 3	39 ± 5
CLL117	Low	107 ± 9	98 ± 7	98 ± 8	97 ± 1	101 ± 7	102 ± 5	84 ± 2
CLL145	Moderate	100 ± 4	107 ± 3	106 ± 6	101 ± 9	84 ± 1	79 ± 1	73 ± 2

Values shown are percentage of untreated controls. Cells were treated with each antibody at 10nM and, where indicated, GAH at 10 μg/mL. The CD20 expression levels of the CLL specimens were provided by Dr Rhona Stein (personal e-mail communication, May 13, 2010).

MTS indicates the viability assay using One Solution assay reagent; and GAH, goat anti–human secondary antibody used for cross linking.

were effective in suppressing the growth of RL and DoHH2 (Figure 1C), as well as CLL specimens (Table 1) from 3 of the 8 patients (CLL078, CLL113, and CLL145) showing higher levels of CD20 expression.[27] It is noted that under the same conditions and even in the presence of GAH, neither rituximab nor veltuzumab showed significant inhibition (10% or less) of CLL samples from all 8 patients.

We next determined whether the observed growth inhibition would involve apoptosis. As shown in Figure 1D, treating Daudi cells for 24 hours with the 3 HexAbs resulted in approximately 20%-30% apoptosis at 10nM, and approximately 25%-35% at 100nM. In contrast, the parental Abs (veltuzumab and epratuzumab) and also rituximab, at 10nM, and epratuzumab at 100nM, did not induce apoptosis beyond the background levels observed with the untreated control. However, a slight increase was observed for the 2 anti-CD20 mAbs, veltuzumab and rituximab, at 100nM. These results confirm our previous findings[25,26] that 20-20, 22-20, and 20-22 are effective in inducing apoptosis without the requirement of a crosslinking Ab, and suggest that apoptosis of Daudi cells may be provoked with higher concentrations of a Type I anti-CD20 mAb,[28] as represented by veltuzumab or rituximab. Similar results were obtained with Raji cells, in which the 3 HexAbs induced approximately 20%-30% apoptosis when tested at 10 or 100nM (data not shown).

Differentiation from anti-IgM and crosslinked anti-CD20

Ligation of the B-cell antigen receptor (BCR) with anti-IgM mAb, or CD20 with veltuzumab or rituximab in the presence of a crosslinking Ab, results in a rapid rise of intracellular calcium.[29] Thus, the inability of the 3 anti-CD20/CD22 HexAbs to affect a notable increase in calcium flux[25,26] suggests the involvement of different signals. Noting that activation of BCR in B cells induces the phosphorylation of Lyn, Syk, and PLCγ2,[30] we first compared the phosphorylation profiles of these key signaling molecules in Daudi cells treated for 24 hours with the following: 133nM of epratuzumab, veltuzumab, or rituximab; 10nM of 20-20, 22-20, or 20-22; or 10 μg/mL of anti-IgM. As shown in Figure 2A, anti-IgM induced the phosphorylation of Lyn, Syk, and PLCγ2 significantly above the basal levels observed for the untreated cells. In contrast, the 3 HexAbs at 10nM neither induced the phosphorylation of Syk nor increased the constitutive level of phosphorylated PLCγ2; however, they effectively reduced the constitutive level of phosphorylated Lyn, which was notable within 2 hours, became more prominent with time, and persisted for at least 24 hours (Figure 2B). Additional studies revealed that the HexAbs diminished the level of phosphorylated Akt (Figure 2C) and stimulated the expression of Raf-1 kinase inhibition protein (RKIP), which was unchanged with anti-IgM (Figure 2D). These characteristic changes were also observed for veltuzumab or rituximab at 133nM (Figure 2A-C), but not at 10nM, as shown for phosphorylated Lyn and Akt (Figure 2E). No appreciable changes were observed with epratuzumab at 10 or 133nM.

Modulation of the MAPK pathways

The up-regulation of RKIP prompted us to investigate whether these anti-CD20/CD22 HexAbs modulate mitogen-activated protein kinase (MAPK) pathways. Intracellular signaling by rituximab has been studied intensively and been reported to influence various signaling pathways in B-cell malignancies,[31-38] in particular, the down-regulation of both phosphorylated extracellular signal regulated kinase (ERK)[33] and p38 MAPK.[38] Daudi cells were treated for

24 hours with 10nM of 20-20, 20-22, or 22-20, or 133nM of epratuzumab, veltuzumab, or rituximab, and whole-cell lysates were subjected to immunoblotting using phosphor-specific ERK and p38 antibodies, with total ERK, p38, and β-actin serving as controls for comparing the amount of proteins loaded in each sample. As shown in Figure 3A, both hexavalent monospecific 20-20 and hexavalent bispecifc 20-22 and 22-20, when tested at 10nM, induced more than a 50% decrease in the levels of phosphorylated ERK, which was also observed with veltuzumab or rituximab at 133nM. In addition, all 3 HexAbs led to a 3-fold increase in the levels of phosphorylated p38, whereas veltuzumab and rituximab appeared to have an opposite or minimal effect on the phosphorylation of p38. Similar results (ie, decrease in phosphorylated ERK and increase in phosphorylated p38) also were observed in Raji cells under the same conditions (data not shown). The time course study in Daudi revealed a continuing decrease of phosphorylated ERK during a 24-hour period, which began to be noticeable at 2 hours after the addition of the HexAbs (Figure 3B). In contrast, crosslinking veltuzumab or rituximab with GAH resulted in enhanced phosphorylation of both ERK and p38 (Figure 3C), thus further attesting that the HexAbs act through different mechanisms from hypercrosslinked anti-CD20 Abs.

NF-κB pathway, Bcl-2 family proteins, and mitochondrial membrane depolarization

Consistent with the observation of increased RKIP and decreased phosphorylation of ERK, which should negatively affect the nuclear factor (NF)-κB pathway, we found a significant reduction in the phosphorylation of IKKα/β and IκBα (Figure 4A). To account for the enhanced potency of the HexAbs to induce

Downloaded from http://ashpublications.net/blood/article-pdf/116/17/3258/1331735/zh804310003258.pdf by guest on 24 May 2024

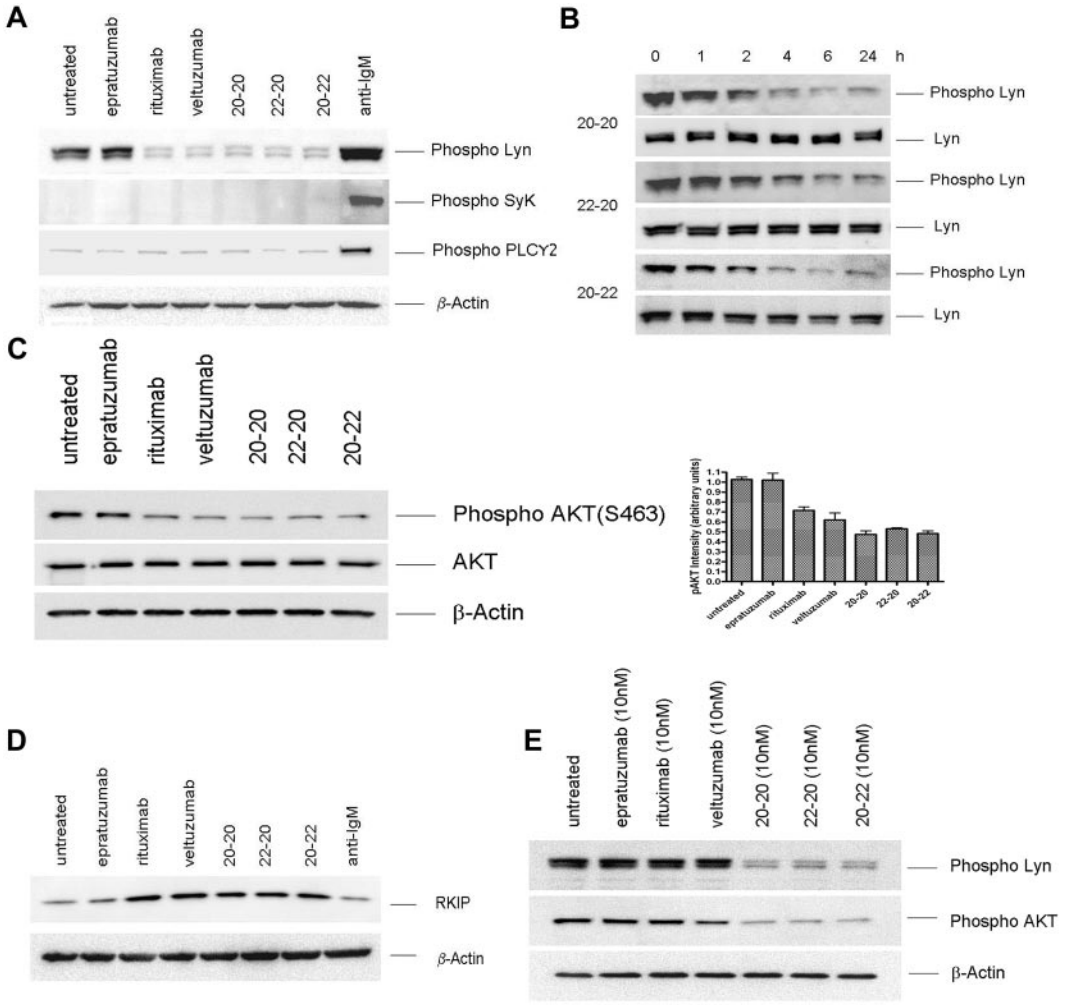

Figure 2. Western blot analysis of select proteins induced in Daudi by the parental antibodies and HexAbs. Parent antibodies each at 133 nM (A,C-D) or 10nM (E); the HexAbs, each at 10nM (A-E); or anti-IgM, at 10 μg/mL (A,C). The changes in phospho-Lyn observed with 20-20, 22-20, and 20-22 within the first 24 hours are shown in panel B.

apoptosis, we also probed the expression levels of certain pro- and antiapoptotic proteins of the Bcl-2 family, and the results (Figure 4B) convincingly demonstrate the down-regulation of at least 4 antiapoptotic proteins (Mcl-1, Bcl-xL, Bcl-2, and phospho-BAD), with concurrent up-regulation of one proapoptotic protein (Bax) that was evident for 22-20 and 20-22. It is noted that the reduction in the antiapoptotic phospho-BAD was not due to a parallel decrease in the apoptotic BAD, which remained unchanged. Such alterations in the balance of anti- and proapoptotic proteins can change the cell fate from survival to apoptosis. The active modulation of Bcl-2 family proteins further led us to determine whether mitochondrial membrane polarization was involved. Surprisingly, only crosslinked veltuzumab or rituximab, but not the HexAbs, could induce an appreciable loss of mitochondrial membrane potential in Daudi cells over the untreated control (Figure 4C), although they were all capable of inducing apoptosis under the conditions examined. These results agree with the notion that the HexAbs differ in mechanisms of action from crosslinked veltuzumab or rituximab.

Role of PTEN

The up-regulation of RKIP as well as the down-regulation of the AKT and NF-κB pathways also prompted us to investigate whether the tumor suppressor, PTEN, plays a specific role in the apoptosis induced by the HexAbs. Daudi cells were treated with 10nM 20-20, 20-22, or 22-20, or with 133nM of rituximab, and the cellular levels of PTEN were examined at 1, 2, 4, 6, and 24 hours (Figure 5A). Whereas all 3 HexAbs induced a notable increase in PTEN at 1 hour, which persisted through the next 3-5 hours and returned to the basal level at 24 hours, no appreciable change in PTEN was observed with rituximab during the same period. Because up-regulation of PTEN may result in enhanced apoptosis, down-regulation of PTEN by specific siRNAs (Figure 5B) should prevent apoptosis, as shown in Figure 5C. The involvement of PTEN was likewise indicated by the observation that LY294002, the specific inhibitor for PI3K, increased the apoptosis induced by the HexAbs from 20% to 25%-40%, but had no effect on either veltuzumab or rituximab (Figure 5D).

Deregulation of cell cycle

The HexAbs were found to arrest Daudi cells in the G_1 phase at both 100nM (Figure 6A) and 10nM (Figure 6B). Treating Daudi cells with veltuzumab or rituximab exhibited a similar distribution of various phases as the untreated cells. The deregulation of cell cycle by the HexAbs was associated with the up-regulation of the CDK inhibitors, as shown for p21, p27(Kip1), and Kip2 in Figure 6C, as well as the down-regulation of cyclin D1 and phosphorylated Rb (Figure 6D).

Downloaded from http://ashpublications.net/blood/article-pdf/116/17/3258/1331735/zh804310003258.pdf by guest on 24 May 2024

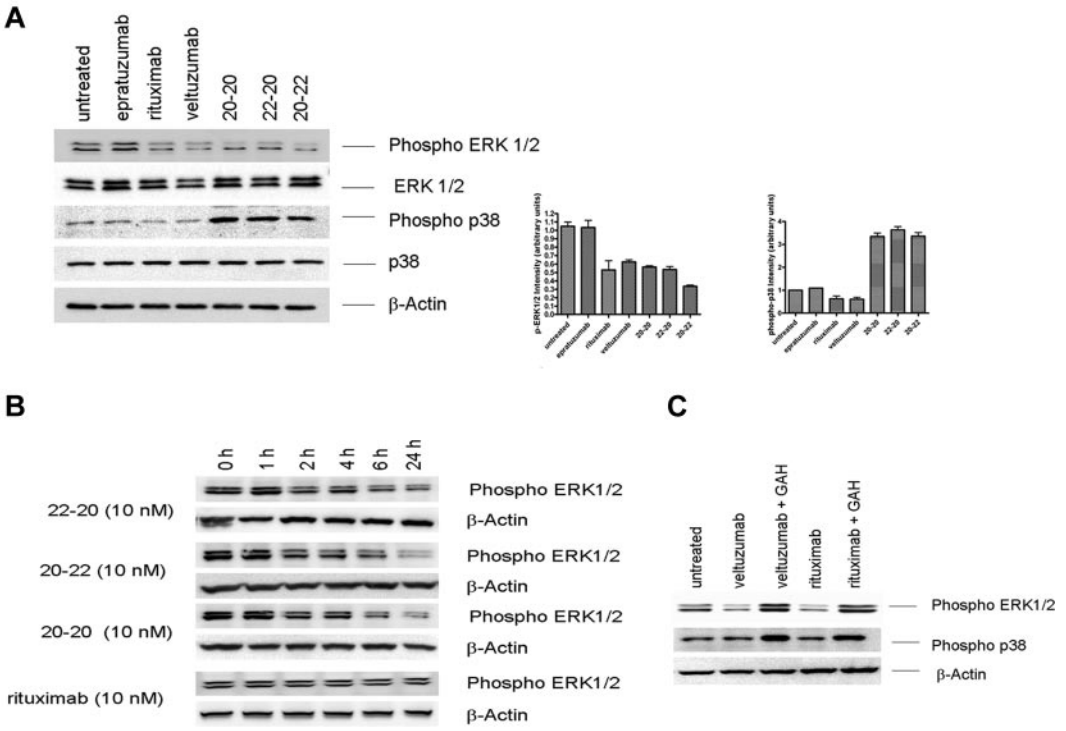

Figure 3. Modulation of ERK1/2 and p38 MAPK pathways. (A) Daudi cells were treated with 133nM each of rituximab, epratuzumab, and veltuzumab and 10nM each of 20-20, 22-20, and 20-22 separately for 24 hours. Cells were immunoblotted and probed with phospho-specific antibodies as well as with antibodies to ERK1/2, p38, and β-actin. Bar diagrams show the relative intensity of phospho-ERK or phospho-p38 induced by each agent, as determined by densitometry analysis of the results from 2 or more independent experiments. (B) Phospho-ERK1/2 induced by 20-20, 22-20, and 20-22 or rituximab at 10nM measured at various time points within the first 24 hours. (C) Up-regulation of phospho-ERK1/2 by crosslinking rituximab and veltuzumab with GAH (10 μg/mL).

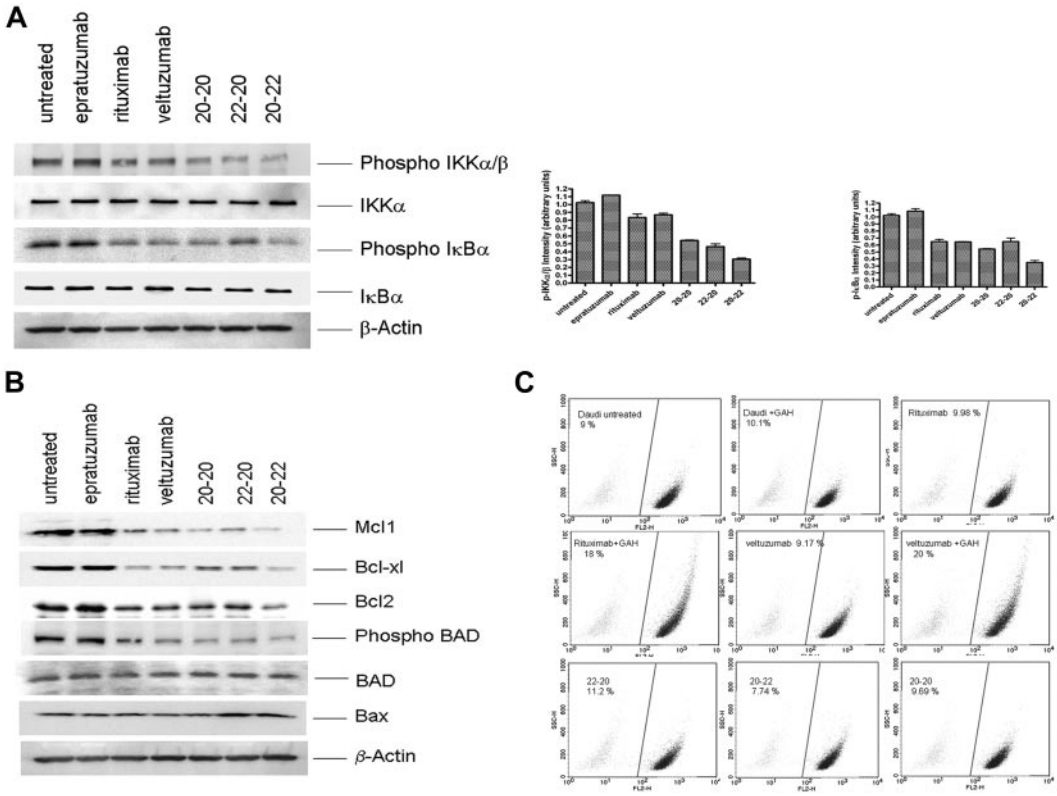

Figure 4. Effects observed in Daudi cells. (A) Selective proteins pertaining to the NF-κB pathway, (B) selective proteins pertaining to the Bcl-2 family, and (C) mitochondrial membrane depolarization.

Downloaded from http://ashpublications.net/blood/article-pdf/116/17/3258/1331735/zh804310003258.pdf by guest on 24 May 2024

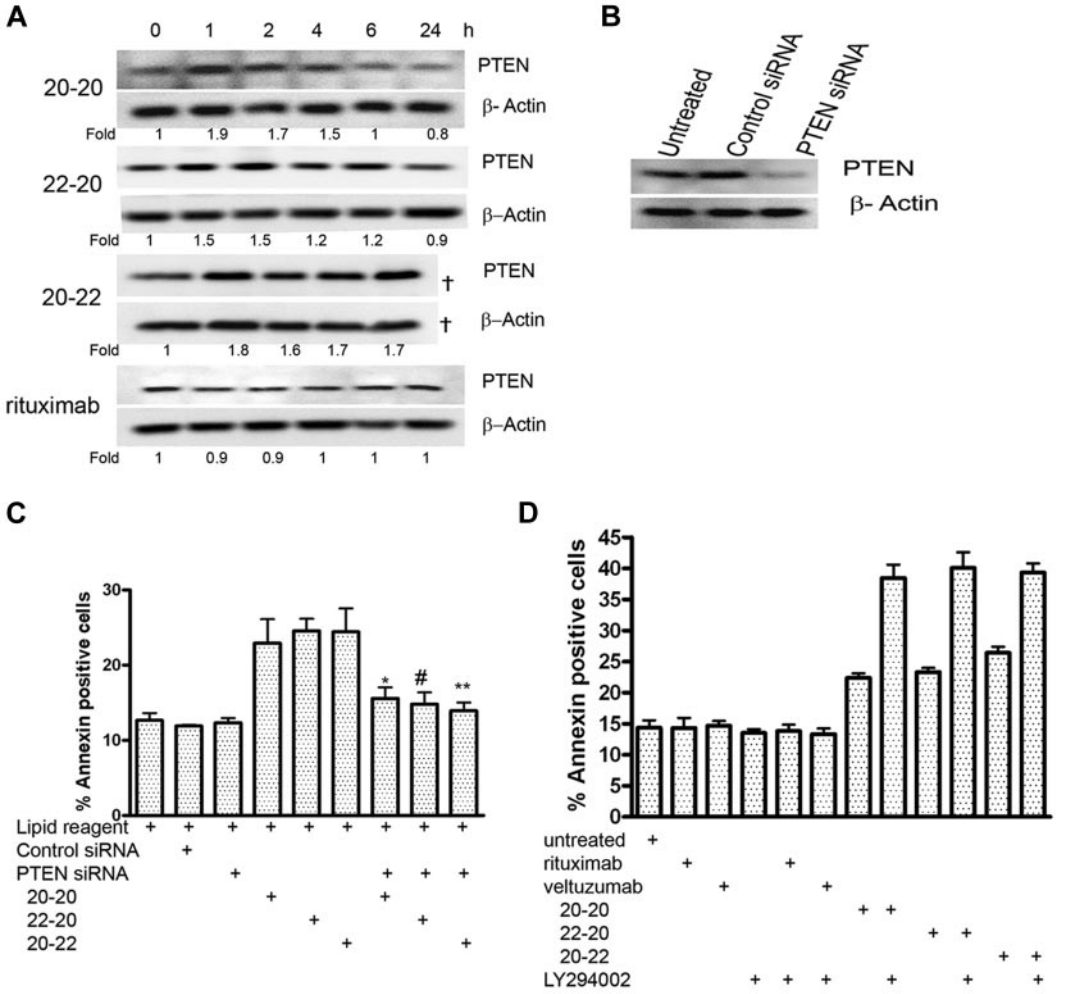

Figure 5. PTEN-PI3K pathway. (A) Time course of PTEN after treating Daudi cells with 20-20, 22-20, and 20-22 at 10nM and rituximab at 133nM. The sample corresponding to 20-22 at 24 hours was lost during loading and thus not analyzed (†). (B) Daudi cells transfected with PTEN siRNA showed reduced expression of PTEN, compared with the untreated cells or cells transfected with control siRNA. (C) PTEN siRNA reduced the apoptosis of Daudi by 20-20, 22-20, and 20-22 at 10nM (*P* values with respect to *20-20, #22-20, and **20-22; $P < .05$). (D) The PI3K inhibitor, LY294002 (5μM), enhanced the apoptosis induced by 20-20, 22-20, and 20-22 at 10nM, but not rituximab at 133nM.

Discussion

The HexAbs (20-20, 20-22, and 22-20) share properties of both Type I (rituximab, veltuzumab) and Type II (B1, tositumomab) mAbs.[28] Consistent with Type II, the HexAbs are negative for CDC and calcium mobilization, do not require crosslinking for growth inhibition or apoptosis, and induce strong homotypic adhesion; yet, they induce translocation of CD20 to lipid rafts as Type I.[25,26] Unexpectedly, 20-20 inhibited proliferation of Burkitt NHL cell lines, Daudi and Raji, in vitro with considerably greater potency, compared with either Type I or II mAbs.[26] Burkitt lymphoma lines, Daudi and Raji, were sensitive to all 3 HexAbs, with similar EC_{50} values[25,26] to crosslinked veltuzumab or rituximab, whereas non-Burkitt lymphoma lines, RL and DoHH2, depicted approximately 25%-40% inhibition on treatment with 10nM HexAbs. The decrease in potency could have been due to the formation of visible clumps by RL and DoHH2 cells in suspension.

Direct toxicity of these HexAbs was also evaluated on 8 CLL patient specimens, which varied in their CD20 expression. The 3 specimens expressing moderate to high CD20 showed 30%-60% inhibition by the HexAbs, whereas no significant inhibition was observed in the other 5 specimens with low CD20 expression. Interestingly, neither rituximab nor veltuzumab, with or without crosslinking, produced measurable inhibition. Although these studies suggest a trend in the activity of HexAbs related to CD20 expression, more patient samples are needed to substantiate this. On the other hand, it is intriguing that these multivalent monospecific/bispecific HexAbs depict better antilymphoma and antileukemia properties than their parental IgGs. Future work will include the investigation of the effects of these HexAbs on rituximab-refractory NHL.

To better elucidate the mechanisms by which direct cell killing is achieved with these hexavalent constructs, we focused here on the investigation of the signaling pathways that are triggered in Daudi cells by the 3 HexAbs, in comparison to those induced by the parental Abs, with some of the experiments repeated in Raji cells. We also performed selective studies in which human lymphoma cells were treated with anti-IgM mAb to activate the BCR, or with veltuzumab or rituximab in the presence of a crosslinking Ab to enhance the apoptotic potency. Our key findings are summarized as follows: (1) The signaling events triggered by 20-20, 22-20, or 20-22 are quantitatively and qualitatively similar in Daudi cells, but distinct from those induced by anti-IgM. (2) Although veltuzumab and rituximab modify the signaling events in Daudi cells similarly to the hexavalent derivatives, as observed for the ERK and NF-κB

Downloaded from http://ashpublications.net/blood/article-pdf/116/17/3258/1331735/zh804310003258.pdf by guest on 24 May 2024

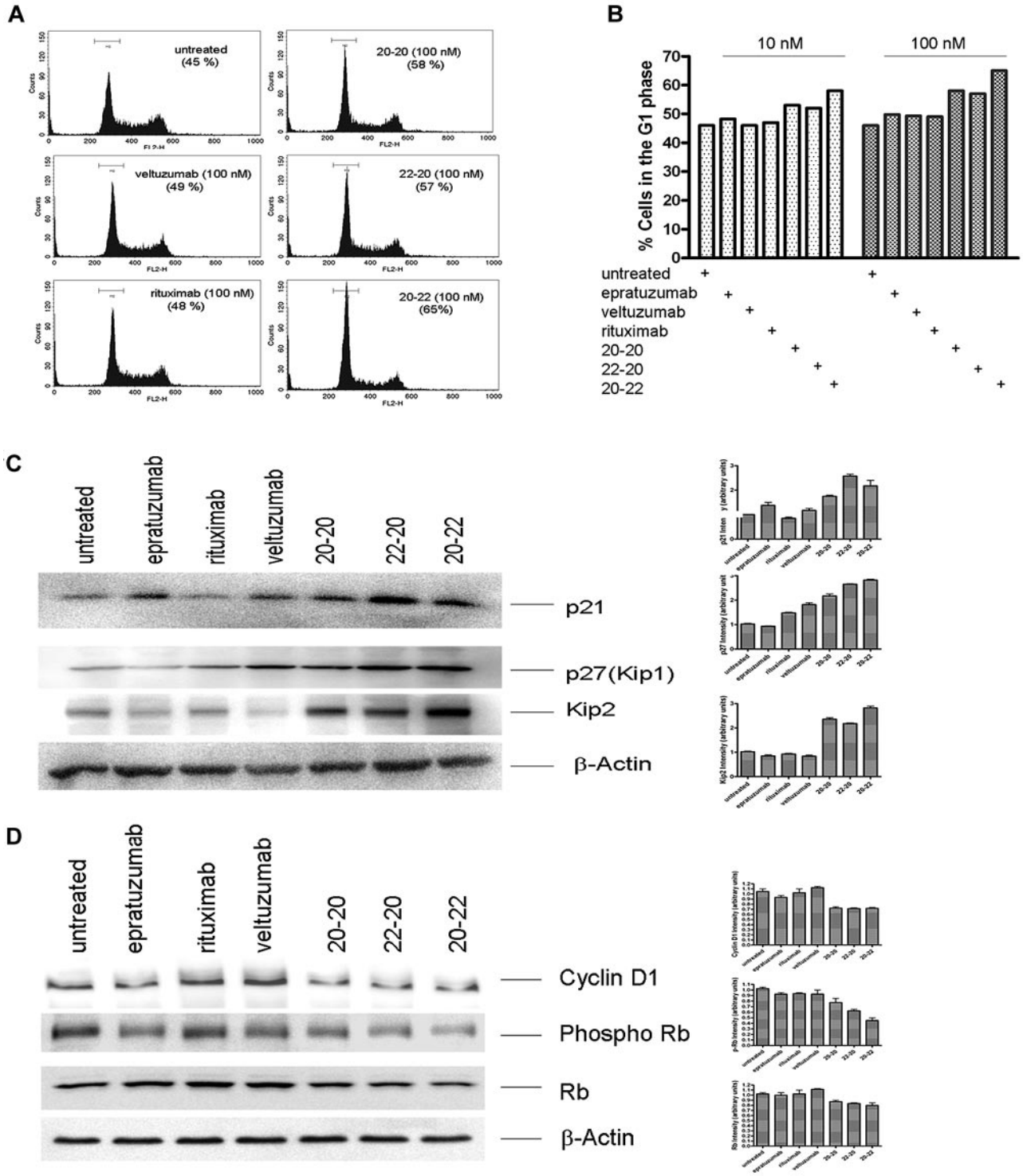

Figure 6. Deregulation of cell cycle. (A) Histograms obtained from Daudi cells treated with 100nM of each agent, showing G_1 arrest induced by 20-20, 22-20, and 20-22. (B) Comparison of cells in the G_1 phase after treatment with each agent at 10 or 100nM. (C) Up-regulation of the Cip/Kip family of proteins on treatment with 20-20, 20-22, and 22-20. (D) Down-regulation of cyclin D1 and p-Rb.

pathways, both require a higher concentration to be effective and are less efficient in modulating the cell-cycle regulators that promote growth arrest. In addition, the bivalent veltuzumab and rituximab fail to alter the levels of phosphorylated p38 and PTEN from untreated control, whereas all 3 HexAbs increase phosphorylated p38 and PTEN levels significantly. Similar results were obtained in Raji cells for the decrease in phosphorylated ERKs and the increase in phosphorylated p38. No appreciable change in the basal expression of signaling molecules was observed in Daudi cells upon ligation of CD22 by epratuzumab. (3) The apoptosis and inhibition of cell proliferation resulting from crosslinking veltuzumab or rituximab with GAH involves signaling events that are distinguishable from those associated with the HexAbs, as manifested in phosphorylated ERK (increase vs decrease), intracellular calcium (increase vs no change), and mitochondrial membrane potential (loss vs no change).

Downloaded from http://ashpublications.net/blood/article-pdf/116/17/3258/1331735/zh804310003258.pdf by guest on 24 May 2024

For example, we showed that all 3 HexAbs at 10nM and the bivalent veltuzumab or rituximab at 133nM, but not at 10nM, produced similar results in the observed levels of various phosphorylated proteins, CDK inhibitors, and Bcl-2 family members that are known to mediate proliferation, cell-cycle arrest, and apoptosis. Specifically, we observed a notable decrease in p-Lyn, p-Akt, p-BAD, p-ERK1/2, p-IKKα/β, p-IKBα, Mcl-1, Bcl-2, and Bcl-xl levels in the treated versus untreated cells, indicating that multiple prosurvival pathways were negatively affected, which require a higher threshold for the bivalent Abs. On the other hand, we also noted that a significant increase in the proapoptotic signals (phosphorylated p38 and Bax), the tumor suppressor (PTEN), and the CDK inhibitors (p21 and Kip2) was only observed with the HexAbs. Moreover, only the HexAbs induced G_1 arrest, which apparently augmented their antiproliferative potency. However, clustering of CD20 or both CD20 and CD22 via the HexAbs induced neither a rapid rise in intracellular calcium nor phosphorylation of Lyn, Syk, and PLCγ, which are characteristic of ligating BCR with anti-IgM.[30] The inability of the HexAbs to effect a transient increase in intracellular calcium as well as a notable $\Delta\psi_m$, and the down-regulation rather than up-regulation of phosphorylated ERK, also differentiate their action from that induced by crosslinking veltuzumab or rituximab with a secondary Ab.

Additional studies using PTEN siRNA and the PI3K inhibitor, LY294002, suggest that PTEN, which converts $PI(3,4,5)P_3$ to $PI(4,5)P_2$, and PI3K, producing $PI(3,4,5)P_3$ from $PI(4,5)P_2$, play opposing roles in mediating the direct toxicity induced by the anti-CD20/CD22 HexAbs, for which we show PTEN siRNA mitigates, whereas LY294002 enhances, the apoptotic outcome. Such results suggest that accumulation of $PI(4,5)P_2$, either via the up-regulation of PTEN or the inhibition of PI3K, may be critical for tipping the balance of survival toward death.

Collectively, our findings are consistent with the view that the potent direct cytotoxicity of 20-20, 22-20, and 20-22 is due to their ability for multivalent binding, which lowers the threshold for modifying multiple signaling pathways, resulting in a new distribution of pro- and antiapoptotic proteins that promotes growth arrest, apoptosis, and, eventually, cell death. Surprisingly, these effects translated to notable differences with regard to their relative potency for killing normal human B cells versus human Burkitt lymphoma cells ex vivo, where 22-20 and 20-22 showed a higher therapeutic ratio (percentage killing of malignant vs percentage normal B cells), compared with veltuzumab and rituximab.[25] Because neither 22-20 nor 20-22 displayed CDC activity, in contrast to the parental veltuzumab, and although 22-20 was less effective in ADCC than 20-22 or veltuzumab, the presence of 4 Fabs of veltuzumab in 22-20 enhanced the ADCC of epratuzumab, which was found to be moderate but statistically significant.[25] Taking into consideration that both 22-20 and 20-22 had a higher therapeutic index ex vivo in terms of relative killing of lymphoma versus normal B cells than their parental mAbs, we speculate that a bispecific anti-CD20/CD22 HexAb may be a more potent class of antilymphoma therapeutic antibodies for clinical use. In terms of treating B-cell lymphomas and leukemias expressing both CD20 and CD22, the results suggest that 22-20, with 4 anti-CD20 Fabs, would be the more effective of the 2 bsAb choices. These experiences stimulate us to study whether bispecific HexAbs against other cancer targets also can acquire different and improved therapeutic properties over their parental bivalent antibody forms.

As reported by Pease et al,[39] the mobility diameter of a Y-shaped monomeric IgG measured by electrospray differential mobility analysis is approximately 9.4 nm, which increases to 11.5 nm for a dimeric IgG, 12.9 nm for a trimeric IgG, and as large as 16.2 nm for an aggregate containing 6 antibodies. Because the length of a Fab is approximately 9 nm and the length of an Fc is approximately 8 nm, we believe the size of HexAbs should not be much larger than a dimeric IgG. Noting that 10-100 nm is considered the optimal range of the diameter for nanoparticle drug carriers in cancer therapy,[40] the concern that a HexAb made by DNL would be too large to penetrate into tumor is likely not valid, but needs to be addressed in further studies.

Acknowledgments

We thank John Kopinski for preparing 20-20, 20-22, and 22-20, and Richard R. Furman, MD, Weill-Cornell Medical College, New York, NY, for providing CLL specimens.

This work was supported in part by National Institutes of Health grant P01-CA103985 from the National Cancer Institute (D.M.G.).

Authorship

Contribution: P.G. designed and performed research, analyzed data, and wrote the manuscript; E.A.R. analyzed data; and D.M.G. and C.-H.C. designed research, analyzed the data, and wrote the manuscript.

Conflict-of-interest disclosure: P.G., E.A.R., C.-H.C., and D.M.G. have employment, stock, and/or stock options with Immunomedics Inc.

Correspondence: Chien-Hsing Chang, Immunomedics, Inc, 300 American Rd, Morris Plains, NJ 07950; e-mail: kchang@immunomedics.com.

References

1. Chames P, van Regenmortel M, Weiss E, Baty D. Therapeutic antibodies: success, limitation and hopes for the future. *Br J Pharmacol.* 2009; 157(2):220-233.
2. Stein R, Qu Z, Chen S, et al. Characterization of a new humanized anti-CD20 monoclonal antibody, IMMU-106, and its use in combination with the humanized anti-CD22 antibody, epratuzumab, for the therapy of non-Hodgkin's lymphoma. *Clin Cancer Res.* 2004;10(8):2868-2878.
3. Tobin E, DeNardo G, Zhang N, Epstein AL, Liu C, DeNardo S. Combination immunotherapy with anti-CD20 and anti-HLA-DR monoclonal antibodies induces synergistically anti-lymphoma effects in human lymphoma cell lines. *Leuk Lymphoma.* 2007;48(5):944-956.
4. Maddipatla S, Hernandez-Ilizaliturriii FJ, Knight J, Czuczman MS. Augmented antitumor activity against B-cell lymphoma by a combination of monoclonal antibodies targeting TRAIL-R1 and CD20. *Clin Cancer Res.* 2007;13(15):4556-4564.
5. Goetsche L, Gonzalez A, Leger O, et al. A recombinant humanized anti-insulin-like growth factor receptor type I antibody (h7C10) enhances the antitumor activity of vinorelbine and anti-epidermal growth factor receptor therapy against human cancer xenografts. *Int J Cancer.* 2005;113(2):316-328.
6. Shang Y, Mao Y, Batson J, et al. Antixenograft tumor activity of a humanized anti-insulin-like growth factor-I receptor monoclonal antibody is associated with decreased AKT activation and glucose uptake. *Mol Cancer Ther.* 2008;7(9): 2599-2608.
7. Nahta R, Hung M-C, Esteva FJ. The HER-2-targeting antibodies trastuzumab and pertuzumab synergistically inhibit the survival of breast cancer cells. *Cancer Res.* 2004;64(7):2343-2346.
8. Leonard JP, Coleman M, Ketas J, et al. Combination antibody therapy with epratuzumab and rituximab in relapsed or refractory non-Hodgkin's lymphoma. *J Clin Oncol.* 2005;23(22):5044-5051.
9. Lu D, Zhang H, Koo H, et al. A fully human recombinant IgG-like bispecific antibody to both the epidermal growth factor receptor and the insulin-like growth factor receptor for enhanced antitumor activity. *J Biol Chem.* 2005;280(20):19665-19672.

Downloaded from http://ashpublications.net/blood/article-pdf/116/17/3258/1331735/zh804310003258.pdf by guest on 24 May 2024

10. Chames P, Baty D. Bispecific antibodies for cancer therapy. *Curr Opin Drug Discov Devel.* 2009; 12(2):276-283.
11. Perez P, Hoffman RW, Shaw S, Bluestone JA, Segal DM. Specific targeting of cytotoxic T cells by anti-T3 linked to anti-target cell antibody. *Nature.* 1985;316(6026):354-356.
12. Glennie MJ, McBride HM, Worth AT, Stevenson GT. Preparation and performance of bispecific F(ab′ gamma)2 antibody containing thioether-linked Fab′ gamma fragments. *J Immunol.* 1987; 139(7):2367-2375.
13. Staerz UD, Bevan MJ. Hybrid hybridoma producing a bispecific monoclonal antibody that can focus effector T-cell activity. *Proc Natl Acad Sci U S A.* 1986;83(5):1453-1457.
14. Kriangkum J, Xu B, Nagata LP, Fulton RE, Suresh MR. Bispecific and bifunctional single chain recombinant antibodies. *Biomol Eng.* 2001; 18(2):31-40.
15. Baeuerle PA, Reinhardt C. Bispecific T-cell engaging antibodies for cancer therapy. *Cancer Res.* 2009;69(12):4941-4944.
16. Coloma MJ, Morrison SL. Design and production of novel tetravalent bispecific antibodies. *Nat Biotechnol.* 1997;15(2):159-163.
17. Shen J, Vil MD, Jimenez X, Iacolina M, Zhang H, Zhu Z. Single variable domain-IgG fusion: a novel recombinant approach to Fc domain-containing bispecific antibodies. *J Biol Chem.* 2006;281(16): 10706-10714.
18. Shen J, Vil MD, Jimenez X, et al. Single variable domain antibody as a versatile building block for the construction of IgG-like bispecific antibdoies. *J Immunol Methods.* 2007;318(1-2):65-74.
19. Asano R, Watanabe Y, Kawaguchi H, et al. Highly effective recombinant format of a humanzied IgG-like bispecific antibody for cancer immunotherapy with retargeting of lymphocytes to tumor cells. *J Biol Chem.* 2007;282(38):27659-27665.
20. Wu C, Ying H, Grinnell C, et al. Simultaneous targeting of multiple disease mediators by a dual-variable domain immunoglobulin. *Nat Biotechnol.* 2007;25(11):1290-1297.
21. Lu D, Zhu Z. Construction and production of an IgG-like bispecific antibody for enhanced therapeutic efficacy. *Methods Mol Biol.* 2009;525:377-404.
22. Rossi EA, Goldenberg DM, Cardillo TM, McBride WJ, Sharkey RM, Chang CH. Stably tethered multifunctional structures of defined composition made by the dock and lock method for use in cancer targeting. *Proc Natl Acad Sci U S A.* 2006; 103(18):6841-6846.
23. Chang CH, Rossi EA, Goldenberg DM. The dock and lock method: a novel platform technology for building multivalent, multifunctional structures of defined composition with retained bioactivity. *Clin Cancer Res.* 2007;13(18):5586s-5591s.
24. Leonard JP, Goldenberg DM. Preclinical and clinical evaluation of epratuzumab (anti-CD22 IgG) in B-cell malignancies. *Oncogene.* 2007;26(25): 3704-3713.
25. Rossi EA, Goldenberg DM, Cardillo TM, Stein R, Chang CH. Hexavalent bispecific antibodies represent a new class of anti-cancer therapeutics: 1. Properties of anti-CD20/CD22 antibodies in lymphoma. *Blood.* 2009;113(24):6161-6171.
26. Rossi EA, Goldenberg DM, Cardillo TM, Stein R, Wang Y, Chang CH. Novel designs of multivalent anti-CD20 humanized antibodies as improved lymphoma therapeutics. *Cancer Res.* 2008; 68(20):8384-8392.
27. Stein R, Gupta P, Chen X, et al. Therapy of B-cell malignancies by anti-HLA-DR humanized monoclonal antibody, IMMU-114, is mediated through hyper-activation of ERK and JNK MAP kinase signaling pathways. *Blood.* 2010;115(25):5180-5190.
28. Cragg MS, Glennie MJ. Antibody specificity controls in vivo effector mechanisms of anti-CD20 reagents. *Blood.* 2004;103(7):2738-2743.
29. Walshe CA, Beers SA, French RR, et al. Induction of cytosolic calcium flux by CD20 is dependent upon B cell antigen receptor signaling. *J Biol Chem.* 2008;283(25):16971-16984.
30. Niiro H, Clark EA. Regulation of B-cell fate by antigen-receptor signals. *Nat Rev Immunol.* 2002;2(12):945-956.
31. Bonavida B. Rituximab-induced inhibition of antiapoptotic cell survival pathways: implications in chemo/immunoresistance, rituximab unresponsiveness, prognostic and novel therapeutic interventions. *Oncogene.* 2007;26(25):3629-3636.
32. Jazirehi AR, Gan XH, De VS, Emmanouilides C, Bonavida B. Rituximab (anti-CD20) selectively modifies Bcl-xL and apoptosis protease activating factor-1 (Apaf-1) expression and sensitizes human non-Hodgkin's lymphoma B cell lines to paclitaxel-induced apoptosis. *Mol Cancer Ther.* 2003; 2(11):1183-1193.
33. Jazirehi AR, Vega MI, Chatterjee D, Goodglick L, Bonavida B. Inhibition of the Raf-MEK1/2-ERK1/2 signaling pathway, Bcl-xL down-regulation, and chemosensitization of non-Hodgkin's lymphoma B cells by rituximab. *Cancer Res.* 2004;64(19): 7117-7126.
34. Jazirehi AR, Huerta-Yepez S, Cheng G, Bonavida B. Rituximab (chimeric anti-CD20 monoclonal antibody) inhibits the constitutive nuclear factor-{kappa}B signaling pathway in non-Hodgkin's lymphoma B-cell lines: role in sensitization to chemotherapeutic drug-induced apoptosis. *Cancer Res.* 2005;65(1):264-276.
35. Jazirehi AR, Vega MI, Bonavida B. Development of rituximab-resistant lymphoma clones with altered cell signaling and cross-resistance to chemotherapy. *Cancer Res.* 2007;67(3):1270-1281.
36. Vega MI, Huerta-Yepez S, Jazirehi AR, Garban H, Bonavida B. Rituximab (chimeric anti-CD20) sensitizes B-NHL cell lines to Fas-induced apoptosis. *Oncogene.* 2005;24(55):8114-8127.
37. Vega MI, Jazirehi AR, Huerta-Yepez S, Bonavida B. Rituximab-induced inhibition of YY1 and Bcl-xL expression in Ramos non-Hodgkin's lymphoma cell line via inhibition of NF-kappa B activity: role of YY1 and Bcl-xL in Fas resistance and chemoresistance, respectively. *J Immunol.* 2005;175(4):2174-2183.
38. Vega MI, Huerta-Yepaz S, Garban H, Jazirehi A, Emmanouilides C, Bonavida B. Rituximab inhibits p38 MAPK activity in 2F7 B NHL and decreases IL-10 transcription: pivotal role of p38 MAPK in drug resistance. *Oncogene.* 2004;23(20): 3530-3540.
39. Pease III LF, Elliot JT, Tsai D-H, Zachariah MR, Tarlov MJ. Determination of protein aggregation with different mobility analysis: application to IgG antibody. *Biotechnol Bioeng.* 2008;101(6): 1214-1222.
40. Davis ME, Chen Z, Shin DM. Nanoparticle therapeutics: an emerging treatment modality for cancer. *Nat Rev Drug Discov.* 2008;7(9):771-782.

Downloaded from http://ashpublications.net/blood/article-pdf/116/17/3258/1331735/zh804310003258.pdf by guest on 24 May 2024